Available online at www.sciencedirect.com
ScienceDirect
Acta Materialia 54 (2006) 4633–4639
Acta MATERIALIA
www.actamat-journals.com

Computational study of heat transport in compositionally disordered binary crystals

John W. Lyver IV [a,b], Estela Blaisten-Barojas [a,*]

[a] Computational Materials Science Center, College of Science, George Mason University, Fairfax, VA 22030, USA
[b] Office of Safety and Mission Assurance, National Aeronautics and Space Administration, Washington, DC 20546, USA

Received 20 March 2006; received in revised form 26 May 2006; accepted 27 May 2006
Available online 24 August 2006

Abstract

The thermal conductivity of compositionally disordered binary crystals with atoms interacting through Lennard-Jones potentials has been studied as a function of temperature. The two species in the crystal differ in mass, hard-core atomic diameter, well depth and relative concentration. The isobaric Monte Carlo was used to equilibrate the samples at near-zero pressure. The isoenergy molecular dynamics combined with the Green–Kubo approach was taken to calculate the heat current time-dependent autocorrelation function and determine the lattice thermal conductivity of the sample. The inverse temperature dependence of the lattice thermal conductivity was shown to fail at low temperatures when the atomic diameters of the two species differ. Instead, the thermal conductivity was nearly a constant across temperatures for species with different atomic diameters. Overall, it is shown that there is a dramatic decrease of the lattice thermal conductivity with increasing atomic radii ratio between species and a moderate decrease due to mass disorder.

Keywords: Binary solids; Compositional disorder; Monte Carlo; Thermal conductivity; Molecular dynamics

1. Introduction

It is known that heat is transported better through solid materials that are pure and crystalline. Any type of impurity, defect, doping or internal boundary within the material nominally increases the resistance to heat transport, and thus reduces the ability to conduct thermal energy. With the growing interest in nanotechnology, the study of thermal conduction properties of systems with reduced dimensions, thin films, nanotubes and superlattices has increased. In nanomaterials and nanostructures, phenomena are highly dependent on the length scale where vibrations between nearest-neighbor atoms occur. The use of molecular dynamics (MD) and the Green–Kubo (GK) methods for calculating the thermal conductivity have shown promise as atomistic approaches for understanding nanosystems at the nanometer scale. For example, there are several recent calculations on pure noble gases with Lennard-Jones interactions and face-centered cubic (fcc) structures in which MD was the method of choice [1–5]. For binary crystals the literature is not so abundant; worth noting is the MD calculation for crystalline β-SiC with point defects [6].

In a crystal the thermal conductivity is composed of two additive contributions: lattice and electronic. The lattice contribution κ_{ph} captures phenomena associated with lattice vibrations and phonon scattering and is dominated by the structural characteristics of the crystal. The electronic contribution κ_e is proportional to the electric conductivity σ_e through the Wiedemann–Franz law [7,8]. The composition of a crystal affects the lattice symmetry characteristics and consequently the lattice vibrations. Therefore, κ_{ph}, the lattice contribution to the thermal conductivity in a crystal, should reflect changes according to its composition. In contrast, since κ_e is a function of σ_e, the conduction properties are expected to remain almost constant for families of solids with similar compositional components. A phenomenon

* Corresponding author. Tel.: +1 703 993 1988.
E-mail address: blaisten@gmu.edu (E. Blaisten-Barojas).

1359-6454/$30.00
doi:10.1016/j.actamat.2006.05.050

that reduces κ_{ph} produces an overall reduction of the thermal conductivity if the electric conductivity is not affected. In dielectrics, and the noble gases specifically, changes in κ_{ph} do not simultaneously affect the electronic conductivity.

This work focuses on simulating the lattice thermal conductivity due to atomic vibrations for binary crystals with compositional disorder. The goal of this work is to identify ranges of combinations of materials and disorder conditions which reduce the lattice thermal conductivity of the simulated binary solid mixtures and may warrant further experimental work. Throughout the remainder of this paper, κ is used to identify the lattice contribution to the overall thermal conductivity.

The effect of compositional disorder on thermal conductivity was investigated using several simple models of binary Lennard-Jones (L-J) solids. Compositional disorder was investigated due to differences in the van der Waal radii (σ), interatomic bond strength (ε) and mass (m) of the two types of atoms. Several relative concentrations of simulated crystalline binary mixtures were studied as a function of selected potential parameters and analyzed across various temperatures. The computational approach taken was to perform atomic-level computer simulations employing a combination of isoenergy MD and NPT Monte Carlo (MC) with a constant number of atoms (N), pressure (P) and temperature (T) to calculate the κ within linear response theory of many-body systems. To validate the work, results were compared to other reported results and experimental data available for monatomic crystals.

This paper is organized as follows. Section 2 describes the methodology used to prepare the binary sample, determine its equilibrium density and allow the sample to reach mechanical equilibrium. Section 3 describes the lattice thermal conductivity results obtained as a function of the parameters used, the lattice disorder models and the various concentrations of the two atomic species. Section 4 concludes the work with a summary.

2. Methodology

A crystalline binary mixture of 500 atoms was simulated in a cubic computational box with periodic boundary conditions in each direction. In the calculations, r_c is the cutoff radius taken as 49% of the width of the computational box. The composition of the binary crystal uses atoms of type "A" as the host and atoms of type "B" as the guest. All parameters were compared relative to the host A atoms. The L-J potential with parameters σ and ε was used as a prototype interaction between atoms. The compositional disorder introduced in the host lattice due to the guest atoms is modeled parameterically by changes of σ, ε and mass. Quantities are expressed in reduced units with respect to the host atoms' L-J parameters σ_A, ε_A and m_A. For example, the mass of Ar is 39.95 a.u. and that of Xe is 131.30 a.u. In reduced units, using Ar as the host atom, the mass of Ar would be 1.0, whereas the mass of Xe would be 3.3. Reduced units of length, energy, temperature, time and thermal conductivity are σ, ε, ε/k_B, $t_o = \sqrt{\sigma^2 m/\varepsilon}$ and $k_B/t_o\tau$, respectively, where k_B is Boltzmann's constant.

Four compositional mixture cases in the computational box were considered with the following characteristics: 100% of pure A atoms, 75% of A atoms and 25% B atoms, 50% of each type, and 25% of A atoms and 75% of B atoms. The L-J parameters for the binary interactions (A–B) are obtained from the combination rules:

$$\sigma_{AB} = \frac{\sigma_A + \sigma_B}{2}; \quad \varepsilon_{AB} = \sqrt{\varepsilon_A \varepsilon_B}. \tag{1}$$

Simulations started at a reduced temperature of 0.5 from a configuration with atoms placed in a perfect fcc lattice. Next, an initial configuration was constructed such that atoms were randomly assigned as type A or B consistent with the relative concentration of the two types of atoms. Throughout this study, to indicate the ratio of parameters, the symbols R_σ, R_ε, R_m are used for σ_B/σ_A, $\varepsilon_B/\varepsilon_A$ and m_B/m_A, respectively. The system was equilibrated by NPT-MC, which allowed for moves of the N atoms in random directions and changes of the entire computational box volume (V). The acceptance criterion between old (V^o) and new (V^n) configurations is given by [9]

$$\begin{aligned}\mathrm{acc}(o \to n) = \min(1, \exp\{-\beta[U(r^N, V^n) - U(r^N, V^o) \\ + P(V^n - V^o) - (N+1)\beta^{-1}\ln(V^n/V^o)]\}).\end{aligned} \tag{2}$$

Here, β is $1/T$, r^N is the vector of the coordinates of all atoms and the potential energy is

$$U(r^N, V) = \frac{1}{2}\sum_i^N \sum_{i\neq j}^N 4\varepsilon_{ij}[(\sigma_{ij}/r_{ij})^{12} - (\sigma_{ij}/r_{ij})^6], \tag{3}$$

where σ_{ij} is the core radius, ε_{ij} is the bond strength and r_{ij} is the interatomic distance of an atomic pair using Eq. (1).

The NPT-MC simulations were run between 1 and 3 million steps with a step being N single atom movements and one volume adjustment. The average density and other calculated quantities were determined as an average over the final one-fourth of the NPT-MC trajectory. Therefore, the position of the atoms within the box is consistent with this average density. The density is defined as N/V irrespective of the two types of atoms, which could have different masses, σ, or ε values. Because the computational box is finite, the value of the pressure was adjusted by subtracting the pressure that would be exerted by a structureless infinite-sized sample outside of the computational box [9].

For the monatomic system, the equilibrium structure was an fcc structure for all temperatures. At low temperatures, no stable amorphous phase was found as obtained in Ref. [3]. Because the NPT-MC calculation does not include the mass in the simulation, the equilibrium ρ for binary samples with A and B atoms having only different ε is the same as the density of the monatomic system. Therefore, the NPT-MC calculations were carried out to determine ρ at different temperatures when $R_\sigma \neq 1$. Fig. 1

shows the temperature behavior of the average ρ for equilibrated systems at zero pressure for samples with a 50:50 relative concentration. The curves correspond to different R_σ. The value of ρ of pure Ar reported in Ref. [3] compares well with our results. As expected, when R_σ increases, the volume must also increase, decreasing ρ. The standard deviation (SD) of the average density is very low, of the order of the symbol size used in Fig. 1. These small fluctuations certainly ensure that the smooth decrease of ρ with temperature illustrated in Fig. 1 is indeed realistic.

The next step was to initiate the isoenergy MD study using the output of the NPT-MC runs. Each MD trial was run 350,000 time steps of $\Delta t = 0.005$ to allow the system first to equilibrate at the desired temperature. Next the MD trial continued to run for half a million time steps to calculate the desired heat current operator values from [10]

$$\vec{J} = \sum_{i=1}^{N} E_i \vec{v}_i + 1/2 \sum_{i=1}^{N} \sum_{j \neq i}^{N} (\vec{v}_i \cdot \vec{F}_{ij}) \vec{r}_{ij}, \tag{4}$$

where E_i is the total energy of each atom, $\vec{v}_i$ is the velocity of each atom and $\vec{F}_{ij}$ and $\vec{r}_{ij}$ are the force and interatomic vectors for each atomic pair.

The next step was to calculate the autocorrelation function $C(\tau)$ of the heat current operator, which is defined as

$$C(\tau) = \langle \vec{J}(\tau + t) \vec{J}(t) \rangle \tag{5}$$

where $\langle\ \rangle$ is the time average, $\vec{J}$ is the heat current operator and τ is the time lag from an origin t chosen from the time trajectory. Each autocorrelation run typically used between 2^{16} and 2^{18} time lags. It was found that for R_σ, R_ε, and R_m near a value of one required longer times to compute the autocorrelation function than when disorder sets in.

The lattice thermal conductivity κ was obtained by integrating $C(\tau)$ over the range $[0, t_{\text{traj}}]$, where t_{traj} is the total time for which the autocorrelation function was calculated. This is the GK approach [11,12]:

$$\kappa = \frac{1}{3Vk_B T^2} \int_0^\infty C(\tau)\, d\tau. \tag{6}$$

The GK approach works well for both amorphous and crystalline models as long as the system is homogeneous. GK takes full account of anharmonic properties but is classical in nature. Ladd et al. [13] were the first to use the GK formalism to calculate thermal conductivity for solids with interactions following an inverse-twelfth power law potential. Later, Gillan extended this method for the study of κ in palladium doped with hydrogen [14]. More recently, Chen et al. used this same approach to study the thermal conductivity of pure Ar doped with Xe [15].

Optimally, it would be best to calculate $C(\tau)$ out to infinity instead of just the finite trajectory length, but this is not possible numerically. We observed that $C(\tau)$ could be approximated by an exponentially decaying cosine function $e^{-\zeta t}\cos(\omega t)$ as shown in Fig. 2 and fit the parameters to the numerical MD results. Then the integration in Eq. (6) was done from the actual simulation data for $0 \leqslant \tau \leqslant t_{\text{fit}}$ and used the decaying cosine function for $t_{\text{fit}} \leqslant \tau \leqslant \infty$. The value of t_{fit} was set to be 1.25 times the period of the fitted cosine function. This time t_{fit} defines the system relaxation time.

The NPT-MC samples prepared in the manner described in previous paragraphs represent different types of compositional disorder. For all values of R_ε or R_m simulated, the structure of the equilibrated sample is the fcc lattice. Thus the system disorder is based on a random mixture of atoms A and B, which are positioned on a perfect lattice. In contrast, when size disorder was introduced with R_σ beyond 1.1, the fcc lattice collapses. This is shown in Fig. 3 which depicts the pair correlation function $g(r)$ in which the $g_{AA}(r)$, $g_{AB}(r)$ and $g_{BB}(r)$ values have been

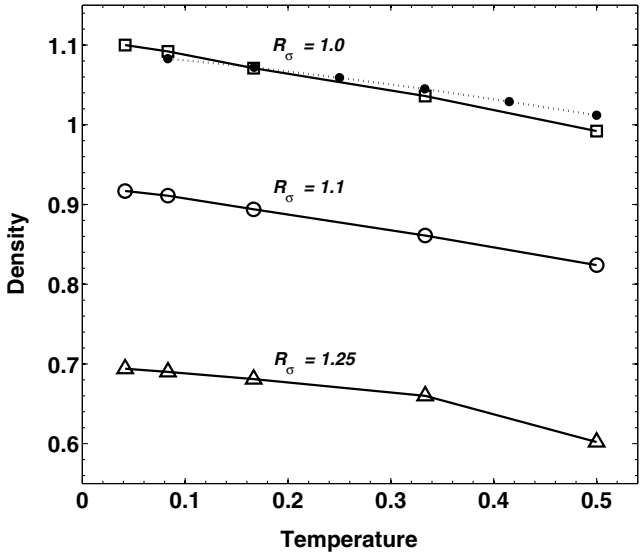

Fig. 1. Density as a function of temperature for radii ratios R_σ of 1.0, 1.1 and 1.25 for the 50:50 mixture of atoms. Crosses are ρ for pure Ar at zero pressure and circles represent results from Ref. [3].

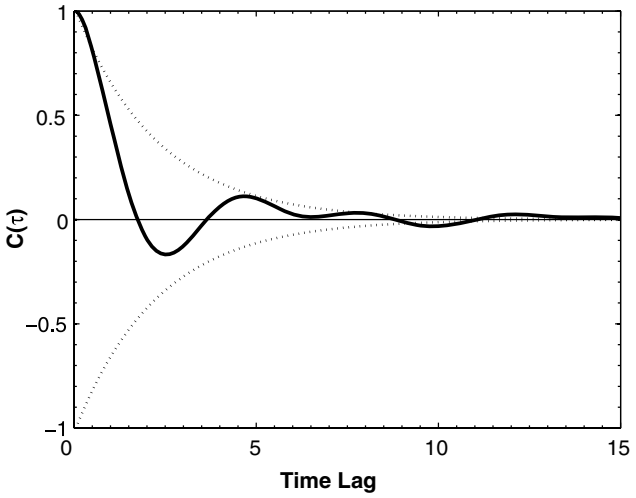

Fig. 2. MD-calculated $C(\tau)$ as a function of time. The dotted lines show the envelope of the exponentially decaying cosine function obtained from the fit of the MD data.

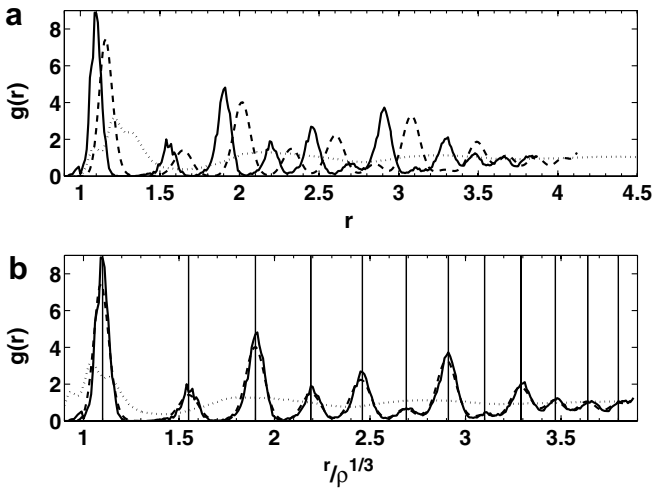

Fig. 3. Radial distribution function $g(r)$: (a) for different R_σ values: 1.0 (solid), 1.1 (dashed) and 1.25 (dotted); (b) same as in (a) plotted as function of scaled distances.

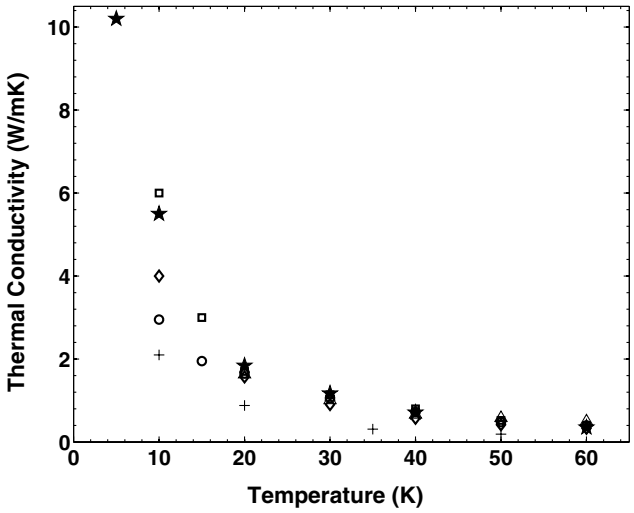

Fig. 4. Thermal conductivity κ as a function of temperature for pure Ar at zero pressure. The results of this work (black stars) are compared to those of other works: Ref. [3] (diamonds), Ref. [15] (circles), Ref. [17] (triangles), Ref. [18] (crosses), Ref. [19] (squares).

summed together. Fig. 3 shows the case of a 50:50 mixture sample at $T = 0.167$ with $R_\varepsilon = 1$, $R_m = 1$ and three different R_σ values (1.0, 1.1 and 1.25). To compare directly between these functions, a scaling of $\rho^{1/3}$ was applied to the radial dependence. It is very clear that for $R_\sigma = 1.25$, the compositional disorder of the 50:50 sample affects the structure very significantly and the crystal collapses into a homogeneous amorphous solid. The structure of this solid amorphous mixture is very different from the structure found in atomic clusters [16], where the atoms with smaller σ segregated and formed a subcluster surrounded by the large σ atoms.

3. Determination of the lattice thermal conductivity

A sample with $N = 500$ at $P = 0$ with only one type of atom was prepared, and κ was obtained for several temperatures using the steps described in Section 2. These results allowed a validation of our method by comparison with several calculations done recently [3,15,17,18] as well as with experimental results [19]. Fig. 4 shows this comparison, indicating that our results (black stars) are in full agreement with previous calculations and with the experimental results.

In the GK approach, Eq. (6), there is an explicit dependence of κ on the volume of the sample. Sample size effects were studied in Ref. [17] where the authors considered computational box sizes containing between 108 and 4000 atoms. Those authors concluded that in the temperature domain of 20–70 K, the size effects are irrelevant for all practical purposes when calculating κ for a pure Ar system. This is consistent with our findings for computational cells containing 108–2048 atoms. It was found that computational boxes smaller than 108 atoms were too small for meaningful results. Fig. 5(a) and (b) illustrates the dependence of the equilibrium density and potential energy averages as a function of the number of fcc cells (n) on each

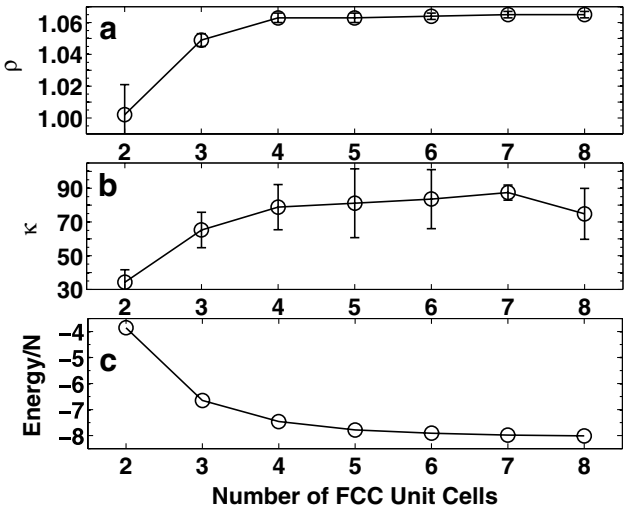

Fig. 5. Effect of computational box sizes. The horizontal axis shows the number of fcc unit cells along each side of the cubic computational box. (a) Density, (b) κ and (c) energy per atom for the ordered monatomic crystal.

computational box edge ($N = 4n^3$). Fig. 5(c) shows κ and its SD as a function of computational box size.

Based on the continued good agreement with both the previously discussed comparisons offset against run times, a system size of $N = 500$ at $P = 0$ was selected for all results reported in this work. The following compositional mixtures were considered: R_σ of 1.0, 1.1, 1.25, 1.5 and 2.0; R_ε of 1.0, 1.25 and 1.5; and R_m of 1.0, 1.6, 2.1 and 3.3. Additionally, we studied different relative concentrations of A and B atoms ranging from 100% A atoms, 75% A with 25% B, 50% A with 50% B, and 25% A with 75% B.

For samples with relative concentrations of 50:50, at a temperature of $T = 0.167$, Fig. 6 illustrates the lattice κ

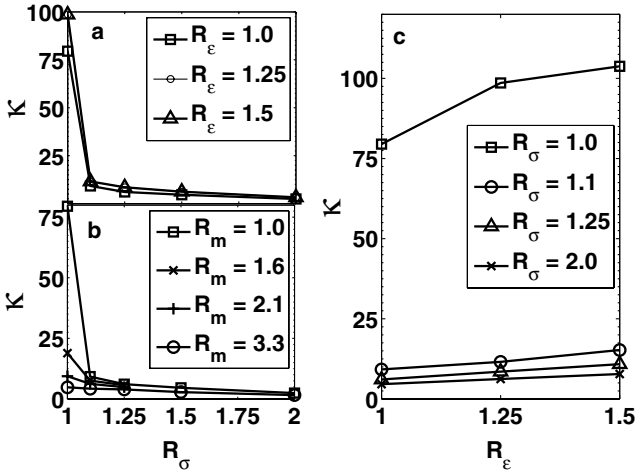

Fig. 6. Thermal conductivity as a function of the parameter ratios: (a) dependence on R_σ for $R_\varepsilon = 1$, 1.25, 1.5, and $R_m = 1$; (b) dependence on R_σ for $R_m = 1$, 1.6, 2.1, 3.3, and $R_\varepsilon = 1$; (c) dependence on R_ε for $R_\sigma = 1$, 1.1, 1.25, and $R_m = 1$.

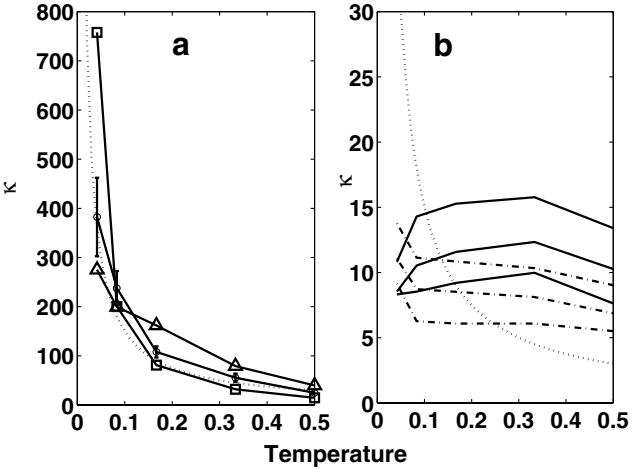

Fig. 7. Thermal conductivity as a function of temperature: (a) structurally ordered case $R_\sigma = 1$, and $R_m = 1$ with $R_\varepsilon = 1$ (squares), $R_\varepsilon = 1.25$ (circles), $R_\varepsilon = 1.5$ (triangles); (b) structurally disordered cases $R_\sigma = 1.1$ (solid lines) and $R_\sigma = 1.25$ (dashed lines). The top, middle and bottom curves are for $R_\varepsilon = 1.0$, 1.25 and 1.5, respectively.

as a function of one parameter ratio (R_σ, R_ε or R_m) while the other two parameter ratios are kept constant. Fig. 6(a) and (b) shows a dramatic decrease of κ with increasing R_σ. In fact, Fig. 6(a) shows that κ decreases by a factor of over 6 between $R_\sigma = 1$ and $R_\sigma = 1.1$ for a constant mass ratio and various values of R_ε. Likewise, Fig. 6(b) shows a dramatic decrease in κ between $R_\sigma = 1$ and $R_\sigma = 1.1$ using different mass ratios. In this case again, κ decreases by factors up to 6 depending upon R_m. While Fig. 6(b) shows a substantial decrease in κ between $R_\sigma = 1$ and $R_\sigma = 1.1$, the two atom types would have to be the same to have $R_\sigma = 1$ and $R_m = 1$, which is a very unrealistic case. On the contrary, Fig. 6(c) shows that, for $R_\varepsilon = 1$ and $R_m = 1$, κ increases slightly as a function of R_σ and increasing R_ε. This increase lies within the SDs of the κ results and might not be a real effect.

The conclusion of the parameter analysis is that at $T = 0.167$, both radii disorder and mass disorder impose a strong depletion of κ. Even a slight difference in atomic radii of only 10% has a major effect on decreasing κ while the mass ratio has a more gradual depleting effect on κ. The mass disorder leaves the crystalline symmetry intact. In comparison, the radii disorder allows the solid to acquire incipient amorphous characteristics as evidenced by the pair correlation function signature illustrated in Fig. 3. In fact for the large difference in atomic radii of 25%, Fig. 3 indicates that the fcc symmetry is already lost and the solid is no longer a crystal.

For monatomic crystalline materials, the expected theoretical dependence of the thermal conductivity with temperature follows an inverse temperature law [7,8]. While previous MD simulations [15] reported κ exhibiting this expected behavior, our results show a departure for any of the proposed samples with disorder. Fig. 7 shows the κ behavior for various values of R_ε of 1.0, 1.25 and 1.5 and $R_m = 1$ for a 50:50 concentration. In Fig. 7 the inverse temperature dependence is plotted with a dotted line to guide the eye. Fig. 7(a) depicts the temperature dependence for $R_\sigma = 1$ with the square, circle and triangle symbols identifying the three values of R_ε (1.0, 1.25 and 1.5), respectively. SDs are shown for the $R_\varepsilon = 1.25$ case and are representative of the other cases. Fig. 7(b) gives results for systems with $R_\sigma = 1.1$ as solid lines corresponding to $R_\varepsilon = 1.0$, 1.25, and 1.5 (top, middle and bottom) and dashed lines for $R_\sigma = 1.25$. SDs are about 1–2 units of κ for all results. It is apparent from these plots that the ordered crystal with no core radius disorder follows the $1/T$ relationship very closely (Fig. 7(a)) while any of the compositionally disordered systems (Fig. 7(b)) present a nearly constant κ as a function of temperature. This degrading of the thermal conduction is similar to that predicted for covalent binary crystals with defects [6] where κ was found to be essentially temperature independent. In our study it should be remembered that compositional disorder in which the atomic radii differ by only 10% produces a dramatic reduction of κ to a minimum value, which keeps fairly constant for the temperatures investigated. In summary, we emphasize that the radii disorder has an extremely strong effect to reduce κ, bringing its value to be a minimum for all calculations with widely varying material parameters.

The last part of this study pertains to changes in the relative concentrations of the A and B atoms. Relative concentrations of A:B atoms of 25:75 and 75:25 were analyzed in addition to the 100% type A and the 50:50 mixture cases discussed above. As the concentration changes, the number of smaller atoms increases relative to the larger atoms having a significant effect on ρ as shown in Fig. 8.

In analyzing mixtures with the 25:75, 50:50 and 75:25 relative concentrations over the range of T, R_σ, R_ε and

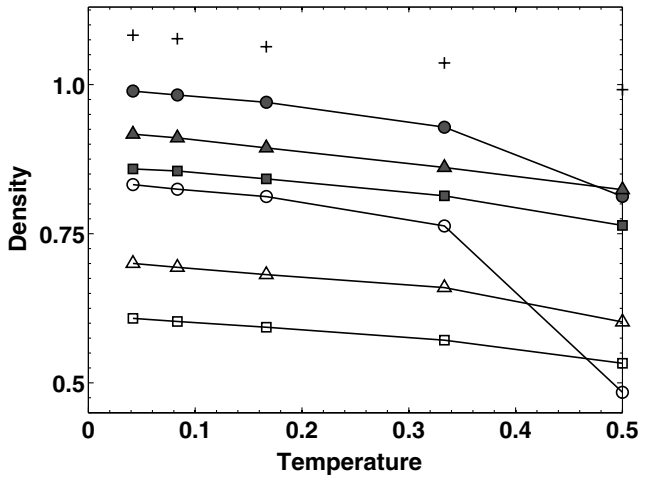

Fig. 8. Density as a function of temperature for different relative concentrations in the mixture. Filled symbols are for $R_\sigma = 1.1$ and open symbols are for $R_\sigma = 1.25$. The circle, triangle and square are for $R_\varepsilon = 1.0$, 1.25 and 1.5, respectively. The case of $R_\sigma = R_\varepsilon = R_m = 1$ is shown as crosses.

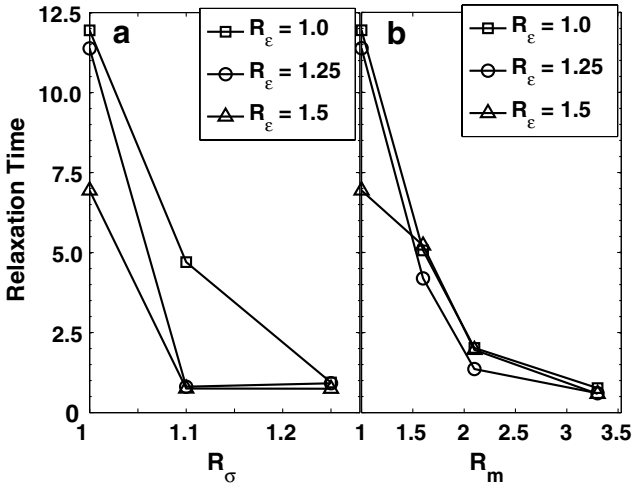

Fig. 9. Relaxation time as a function of parameter ratios for the 50:50 sample: (a) dependence on R_σ with $R_m = 1$ and $R_\varepsilon = 1$ (squares), 1.25 (circles), 2.5 (triangles); (b) dependence on R_m with $R_\sigma = 1$ and three R_ε values as in (a).

R_m, the behavior of κ was very similar to that of the 50:50 case. Table 1 summarizes all results of κ for the various disorder cases at five temperatures. Once again, for these relative concentrations studied, the maximum decrease in κ is through R_σ.

Additionally, as is shown in Fig. 6(c) for the 50:50 relative concentrations, the effect of increasing R_ε while R_σ and R_m remain constant, produced an apparent slight increase in κ. This effect is also present for the other relative concentrations as reported in Table 1.

To compute the lattice thermal conductivity from Eq. (6), the autocorrelation function $C(\tau)$ was approximated by an exponentially decaying cosine function. In Fig. 9, the vertical axis on both plots depicts the system relaxation time and is plotted as a function of R_σ in Fig. 9(a) and R_m in Fig. 9(b). The relaxation time appears to be directly related to the amount of core radii and mass disorder present in the sample. The change in relaxation time due to the ε disorder is small as evidenced by the three curves in Fig. 9(a) and (b).

Table 1
Lattice thermal conductivity for solid mixtures with various relative concentrations and at $T = 0.042$, 0.083, 0.167, 0.333 and 0.500 (top to bottom in each table entry)

Relative concentration	$R_\sigma = 1$, $R_m = 1$, $R_\varepsilon = 1$	R_σ		R_ε		R_m		
		1.1	1.25	1.25	1.5	1.6	2.1	3.3
100% A	476.6							
	200.1							
	79.5							
	31.9							
	14.5							
75% A, 25% B		8.8	5.8	331.5	184.2	–	–	–
		9.5	7.1	201.1	138.8	–	–	–
		10.4	6.6	98.9	75.4	22.9	12.4	7.2
		10.6	6.0	37.4	35.8	–	–	–
		6.8	3.2	16.8	18.1	–	–	–
50% A, 50% B		8.3	9.1	329.4	230.1	–	–	–
		8.5	6.3	193.2	164.7	–	–	–
		8.4	6.0	98.4	113.1	18.9	9.4	4.8
		10.0	6.1	41.8	49.9	–	–	–
		7.6	5.5	23.5	26.2	–	–	–
25% A, 75% B		7.5	9.4	231.2	275.1	–	–	–
		9.0	6.2	331.8	199.6	–	–	–
		16.9	6.3	107.9	141.3	22.8	14.7	3.6
		11.2	5.8	55.3	79.1	–	–	–
		8.5	5.4	24.6	39.8	–	–	–

For any parameter ratio $\neq 1$, the other two parameter ratios $= 1$. Values are in reduced units.

4. Summary and conclusions

Throughout this work, it has been shown that studying the effects of radii, mass, interatomic interaction disorder and temperature can be demonstrated in a computer-simulated environment. Our work was performed on a PC with a single Pentium 4 processor (3.2 GHz) and each NPT-MC and MD run consumed about 9 and 4 h of processing time, respectively, per data point, making the work reasonable to accomplish.

The results of this work show that compositional disorder at the nanoscale in crystalline binary mixtures decrease the lattice thermal conductivity in a dramatic fashion. Findings in this work are important for tailoring the synthesis of new materials with poor heat conduction characteristics. The relative properties of L-J solid mixtures are summarized below in order of importance for degrading the lattice thermal conductivity:

(1) *van der Waal radii.* Atoms should have different radii. Even a 10% difference brings the lattice thermal conductivity to a minimum constant value and suppresses the inverse temperature depletion. The reason for the dramatic degradation of the heat conduction is the additional phonon scattering imposed at the nanoscale by atoms that are at the threshold of collapsing the crystal structure of the solid.
(2) *Mass.* Atoms should have different masses. Differences of 60% in mass decrease the thermal conductivity by about half at any temperature below the melting point.
(3) *Interatomic interaction strength.* Atoms should have almost equal values. With a 50% difference in strength, thermal conductivity can be increased by about 25%, which is not a desired outcome.
(4) *Temperature.* Temperature is a key factor for any application searching to deplete heat conduction due to atomic vibrations. This work was done for reduced temperatures of up to 0.5, which are below the meting points of the L-J compositionally disordered crystals studied. In this temperature range, when radii disorder exists, the lattice thermal conductivity is essentially temperature independent and markedly degraded due to the enhanced phonon scattering induced by atoms with different radii placed randomly on an fcc crystal.
(5) *Composition relative concentration.* Relative concentration of the two components in the crystal appears to have only a minor effect on the thermal conductivity.

References

[1] Lukes JR, Dy L, Liang X-G, Tien C-L. Trans ASME 2000;122:536–43.
[2] Feng X-L, Li Z-X, Guo Z-Y. Chin Phys Lett 2000;18:416–9.
[3] McGaughey AJH, Kaviany M. Int J Heat Mass Transf 2004;47:1783–98.
[4] Chen Y, Li D, Yang J, Wu Y, Lukes JR. Physica B 2004;349:270.
[5] Heino P. Phys Rev B 2005;71:144302.
[6] Li J, Porter L, Yip S. J Nucl Mater 1998;255:139–52.
[7] Berman R. Thermal conduction in solids. Oxford: Clarendon Press; 1976.
[8] Jonson M, Mahan GD. Phys Rev B 1980;21:4223–9.
[9] Frenkel D, Smit B. Understanding molecular simulation. New York (NY): Academic Press; 1998.
[10] Balescu R. Equilibrium and non-equilibrium statistical mechanics. New York (NY): Wiley; 1979 [Chapter 21].
[11] Green MS. J Chem Phys 1952;20:1281–95;
Green MS. J Chem Phys 1954;22:398.
[12] Kubo R. J Phys Soc Jpn 1957;12:570–86.
[13] Ladd AJC, Moran B, Hoover WG. Phys Rev B 1986;34:5058–64.
[14] Gillan MJ. J Phys C Condens Matter 1987;20:521–38.
[15] Chen Y, Lukes JR, Yang J, Wu Y. J Chem Phys 2004;120:3841–6.
[16] Garzon IL, Long XP, Kawai R, Weare JH. Chem Phys Lett 1989;158:525–30.
[17] Tretiakov KV, Scandolo S. J Chem Phys 2004;120:3765–9.
[18] Kaburaki H, Li J, Yip S. Matter Res Soc Symp Proc 1998;538:503–8.
[19] Christen DK, Pollack GL. Phys Rev B 1975;12:3380–91.